Structural Study of Cu/Co Multilayer by Anomalous Small-Angle X-ray Scattering

Structural Study of Cu/Co Multilayer by Anomalous Small-Angle X-ray Scattering*

Eiichiro Matsubara and Yoshio Waseda
Institute for Advanced Materials Processing
(Received February 12, 1993)

Synopsis

The diffraction peaks in the small-angle region due to a long period of a Cu/Co multilayer were observed with the anomalous small-angle x-ray scattering in reflection geometry. These peaks appear to be enhanced because of a large negative value of the real part of the anomalous dispersion term of Co just below the Co K-absorption edge. By comparing the relative integrated intensities of these peaks with the theoretical values calculated from a trapezoidal concentration model, the concentration profile along the surface normal in this multilayer has been determined.

I. Introduction

Synthetic multilayered structures have received much attention, because of their scientific and technological potentials. Soft x-ray monochromators are one of the well known applications. In such a case, elements with large and low atomic numbers like Si or C and W, are alternately stacked with a certain periodic thickness for obtaining large scattering power. On the other hand, the development of magnetic multilayers has recently grown very rapidly. Especially, the gigant magnetoresistance has been intensively studied since the gigant magnetoresistance was discovered in Fe/Cr multilayers[1]. Recently, in Co/Cu multilayers prepared by ultrahigh-vacuum sputtering, the magnetoresistance ratio was found as large as 78% at 4.2K and 48% at room temperature[2,3]. In addition to the gigantic magnetoresistance, these multilayers show the antiferro- and ferro-magnetic oscillation behavior with increase in thickness of the non-magnetic layers[2,3]. The origin of these peculiar features has not been well understood yet. Thus, not only the magnetic measurements but also the structural investigations are strongly required.

Small-angle x-ray diffraction in reflection geometry has been used for characterizing multilayer structures in various systems. Sharp diffraction peaks due to their periodic layered structure of different kinds of elements provide us information about the periodicity, thickness of the individual layers and the concentration profile across the interface. Their peak intensities are proportional to the difference between the average x-ray atomic scattering factor of each layer. Since the elements forming the gigant

---

* The 93 R-1*th* report of Institute for Advanced Materials Processing.

magnetoresistance multilayers have close atomic numbers, e.g. Cr, Mn, Fe, Co, Ni and Cu, only weak diffraction peaks are expected in the small-angle region. The anomalous x-ray scattering (AXS) effect is undoubtedly useful tool in order to enhance a contrast of x-ray scattering power between the layers. Nakayama et al[4] studied the structure of the interface in the Fe/Mn multilayer with this AXS method.

Similarly, in the present study, the AXS effect below Co K-absorption edge was applied to the structural study of a Cu/Co multilayer. A full detail of the derivation of equations used in the present analysis will also given including the results of the AXS measurements in the Cu/Co multilayer.

II. Experimental

A Co/Cu multilayer was deposited on a MgO (110) single-crystal substrate at room temperature by the ion beam sputter deposition method, with Co and Cu metal disks as target. Cu and Co layers of 1.0 nm thick are alternately stacked with 50 periods. The details of the sample preparation were explained in elsewhere[5].

Anomalous x-ray scattering intensities were measured at BL-6B at the Photon Factory (PF) of National Laboratory for High-Energy Physics, Tsukuba, Japan. The experimental setting is schematically shown in **Figure 1**. The incident beam energy was selected by the Si (111) double crystal monochromator. The incident beam intensity was monitored by the ionization chamber placed just in front of the sample. The sample was mounted on the vertical double-axis diffractometer so that correction for the polarization effect was ignored. Scattering intensities were measured at 7.686 keV, which is 25 eV below Co K-absorption edge. The second crystal of the double crystal monochromator was slightly detuned in order to reduce the intensity of the higher harmonics of $\lambda/3$ reflected by Si (333) to an insignificant level. At this energy, a small amount of the Co fluorescent radiation which was

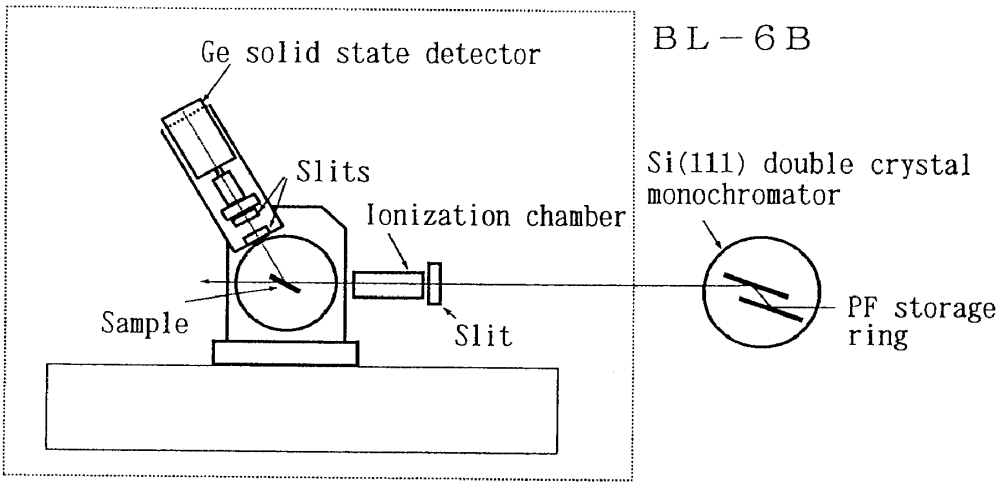

Figure 1 Schematic diagram of the experimental setting for the anomalous small-angle x-ray scattering measurement in reflection geometry at the Photon Factory, Tsukuba, Japan.

mainly caused by the tail of the band pass of the monochromator was observed. Since it is known that separation of this fluorescent radiation from the elastic intensity is crucial to obtain reliable anomalous x-ray scattering data, the Co Kα radiation was separately collected from the elastic intensity by a portable pure Ge solid state detector. Using the tabulated ratio of Co Kβ to Co Kα fluorescent radiations[6] and the observed Co Kα radiation, the Co Kβ radiation overlapping with the elastic scattering was corrected. The details of the AXS measurements at PF were already given in elsewhere[7].

The power of the incident beam for a certain time ($t_m P_o$) is related to the total monitor count by the ionization chamber in Figure 1 (I_m) for the time t_m.

$$t_m P_o = (E_p I_m / E e G_a G_v) \exp(-\mu_a r_i) \exp(-\mu_i (l_t + l_e)/2) / \{1 - \exp(-\mu_i l_e)\} \quad (1)$$

where E_p is the energy to form an ion-electron pair, E the energy of incident photons and e the electron charge. μ_i and μ_a are the linear absorption coefficients of gas for the ion chamber and air, and G_a and G_v the gain of the current amplifier and the conversion gain of the voltage-frequency converter. l_t , l_e and r_i are the total length of the ion chamber, the length of the electrode in the ion chamber and the distance from the ion chamber to the sample, respectively. The observed intensity I_{obs} is given, using Eq (1) for $t_m P_o$,

$$I_{obs}(Q,E) = C\ P\ A_s\ (\rho_s / M_s)\ I_{eu}(Q,E) \quad (2)$$

where

$$C = t_m P_o\ (e^4/m^2c^4)\ (wh/r_d^2)\ N_A \quad (3)$$

$$A_s = \frac{1}{2\mu_s}\ [1 - \exp(-\frac{2\mu_s t_s}{\sin\theta})] \quad (4)$$

$$P = \frac{1}{\sin 2\theta} \quad (5)$$

$Q=|Q|=4\pi\sin\theta/\lambda$, 2θ is the scattering angle and λ the wavelength. P is the Lorentz-polarization term, N_A Avogadro's number, m the electron rest mass and c the velocity of light. w and h are the width and height of the diffracted beam on the counter and r_d is the distance from the sample to the counter. The terms of μ_s, ρ_s, M_s and I_{eu} are the linear absorption coefficient, density, atomic weight and scattering intensity in absolute units, respectively. In the present case, the values averaged over pure Cu and Co metals are used for the parameters of μ_s, ρ_s and M_s. By using Eq.(2), the observed intensity is converted into the absolute scale. In this way, the converted intensities observed at different energies are compared with each other in the same scale.

III. Theoretical Background

The stepwise concentration profile along the surface normal is the simplest model for multilayers. This is, however, often apart from the actual profiles. In the present study, the trapezoidal concentration profile shown in **Figure 2** is assumed. The horizontal and vertical axes correspond to a distance x along the surface normal and an atomic concentration of Cu, $C(x)$, respectively. In this figure, two layers labelled "A" and "B" are alternately stacked along x with a period of L and a linear concentration gradient with a thickness of t is assumed between these two layers. For convenience of the following discussion, the regions I, II, III and IV are defined as seen in the figure. The parameters of C_A and C_B indicate the Cu concentrations in the A and B layers.

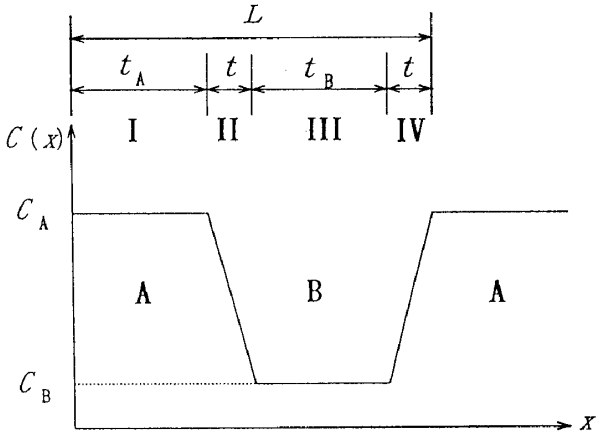

Figure 2 A Cu concentration profile ($C(x)$) in the trapezoidal model of the Cu/Co multilayer.

The structural factor for a Cu/Co multilayer with the concentration profile $C(x)$ is given by

$$F(Q) = \{n_A(C_A f_{Cu}+(1-C_A)f_{Co}) - n_B(C_B f_{Cu}+(1-C_B)f_{Co}\} \int_0^L C(x)\exp(iQx)\,dx \tag{6}$$

where f_{Cu} and f_{Co} are the x-ray atomic scattering factors of Cu and Co, n_A and n_B the number densities of the A and B layers. The trapezoidal Cu concentration profile in Figure 2 is given as follows.

$$\begin{aligned} C(x) &= 1 && \text{for } 0 \le x \le t_A && \text{(Region I)} \\ &= 1-(x-t_A)/t && \text{for } t_A \le x \le t_A+t && \text{(Region II)} \\ &= 0 && \text{for } t_A+t \le x \le t_A+t_B+t && \text{(Region III)} \\ &= \{x-(t_A+t_B+t)\}t && \text{for } t_A+t_B+t \le x \le L && \text{(Region IV)} \end{aligned} \tag{7}$$

The relation between the layer thicknesses of t_A, t_B and t are obtained from the conservation law of the total Cu concentration. That is,

$$(C_A-C_B)\,t_A = (1-C_B)\,t_A^o - C_B\,t_B^o - (C_A-C_B)\,t \tag{8}$$

$$(C_A-C_B)\,t_B = -(1-C_A)\,t_A^o + C_A\,t_B^o - (C_A-C_B)\,t \tag{9}$$

In Eqs.(8) and (9), C_A=1 for C_B=0. Thus, the following simple relation is derived.

$$t_A = t_A^o - t, \quad t_B = t_B^o - t \tag{10}$$

On the assumption that n_A is nearly equal to n_B, substitution of the concentration profile $C(x)$ in Eq (7) and the relations in Eq (10) into Eq (6) gives the structure factor $F(Q)$. Thus, the scattering intensity of the multilayer in electron units per atom, I_{eu}, becomes

$$I_{eu}(Q) = F(Q)F^*(Q)\frac{\sin^2(NQL/2)}{\sin^2(QL/2)} \tag{11}$$

$$\begin{aligned} F(Q)F^*(Q) = {} & n^2(C_A - C_B)^2 |f_{Cu} - f_{Co}|^2 \; [(2/Q^2)(1-\cos QL) \\ & + (2/tQ^3)\{\sin Q(t_A^o - t) - \sin Qt_A^o - \sin Q(L-t) + \sin QL + \sin Q(L-t_A^o+t) - \sin Q(L-t_A^o) - \sin Qt\} \\ & + (4/t^2Q^4)\{1 - \cos Qt - \cos Q(L-t_A^o) + \cos Q(L-t_A^o+t)\}] \end{aligned} \tag{12}$$

$$|f_{Cu} - f_{Co}|^2 = \{(f_{Cu}^o + f_{Cu}') - (f_{Co}^o + f_{Co}')\}^2 - (f_{Cu}'' - f_{Co}'')^2 \tag{13}$$

where f' and f'' are the anomalous dispersion terms and f^o is the ordinary x-ray atomic scattering factor. The term of F^* is the complex conjugate of F. The term N is the total number of periods. The last sine function in Eq (11) is called the Laue equation which have a sharp maximum when $Q=2\pi l/L$. The structure factor FF^* varies these $00l$ peak intensities. Equation (11) is also described using the ratio of the initial thicknesses of the A and B layers.

$$r_{BA} = t_B^o / t_A^o \tag{14}$$

Using the period L and Eq (14), the initial thickness of each layer is expressed by

$$t_A^o = L/(1+r_{BA}), \quad t_B^o = r_{BA}L/(1+r_{BA}) \tag{15}$$

Substituting Eq (15) for t_A^o in Eq (11), the peak intensities are also described as a function of t, C_A and r_{BA}. The peak intensities change with these parameters in different ways.

Let me apply this equation to the present Cu/Co multilayer. **Figure 3** shows the dependence of the scattering intensities of the first 4 ($00l$) peaks upon the Cu concentration of the A layer, C_A, when the thickness ratios r_{BA} are 1.0 and 1.2. The Cu concentration of the B layer, C_B, is computed by the following relation equivalent to Eq (8).

$$C_B = (1 - C_A)/r_{BA} \tag{16}$$

All of the peak intensities monotonically decrease with C_A without changing their relative intensities. In other words, as long as the relative peak intensities are concerned in the analysis, the information about the Cu concentration in each layer is completely not detected. It is also notified that the peaks

with even indices are not observed in the case of r_{BA}=1. Similarly, the peak intensities computed with various t-values for r_{BA}=1 are shown in **Figure 4**. The peak intensities decrease with increase in the thickness of t and the 003 peak intensity is reduced more rapidly than the 001 peak intensity. The peak intensities of 002 and 004 peaks are still equal to zero in spite of the presence of the concentration gradient. Finally, when the ratio of the initial layer thicknesses is changed from 0.5 to 1.5, the peak intensities are changed as shown in **Figure 5**. The layer thicknesses for the A and B layers, t_A and t_B were computed at various r_{BA}, using Eqs (10) and (15). The peak intensities vary with r_{BA} in a complicated manner than those in Figures 3 and 4. In Figure 5, the peak intensities are calculated at two energies of 25 eV below Co K-absorption edge and 220 eV above Cu K-absorption edge. The difference of the peak intensities at these two energies will be discussed later.

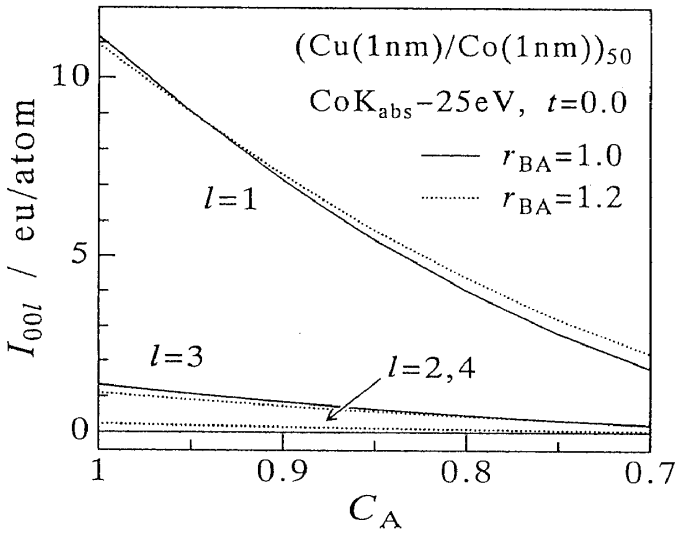

Figure 3 Intensities of the first 4 (00l) peaks for the Cu/Co multilayer as a function of the Cu concentration of the A layer when t=0, and r_{BA}=1.0 (solid) and 1.2 (dotted).

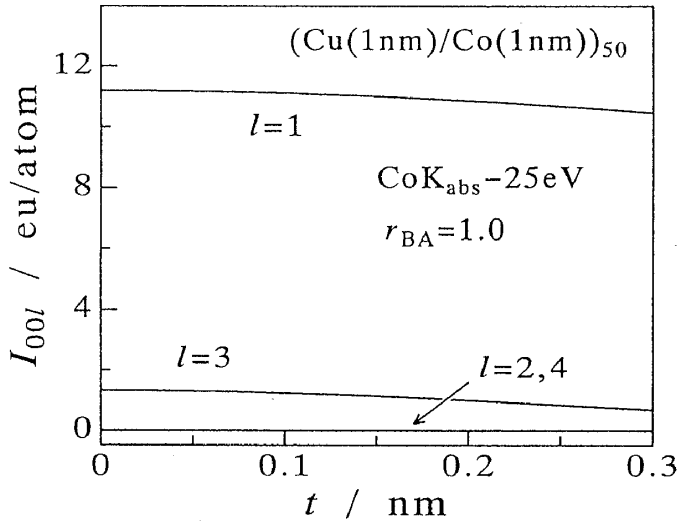

Figure 4 Intensities of the first 4 (00l) peaks for the Cu/Co multilayer as a function of the thickness of the transition layer t when C_A=1 and r_{BA}=1.0.

IV. Results and Discussion

The peak intensities of the Cu/Co multilayer observed at energy of 25 eV below Co K-absorption edge are shown in **Figure 6**. Four peaks are observed in the present measurement. Since the 004 peak indicated with an arrow is not well resolved, the period of L is computed from the positions of the first 3 peaks, taking account of a peak shift at small angles, that is,

$$2\theta=2\theta_B+4\delta/\sin 2\theta_B \quad (17)$$

where $2\theta_B$ and 2θ are the actual and apparent scattering angles, and δ is the dispersion part of the complex refractive index. In the present case, $\delta=2.47\times10^{-5}$. The period becomes 2.083±0.003 nm. The integrated intensities of these four peaks are estimated by subtracting a smooth background. As mentioned in Figures 3 and 4, the peaks with even indices, i.e. 002 and 004, are not present when the A and B layers have an equal thickness. Thus, the presence of the 002 peak suggests that r_{BA} is not exactly equal to 1. In order to obtain a model of the present Cu/Co multilayer, the parameters of r_{BA}, t and C_A are determined so that the experimental relative intensities for the first 3 peaks are successfully explained by the calculated values in Eq (11). When t=0.00±0.01nm, r_{BA}=1.2±0.05 and C_A=1.0, the experimental values coincide with the calculated ones. The results are summarized in **Table 1**. As mentioned in the previous section, the structural analysis with the relative intensities does not give any information about the parameter C_A. However, since there is no concentration gradient between the A and B layers i.e. t=0.0 nm, it is more likely that the A and B layers are pure Cu and Co, i.e. C_A=1.0 and C_B=0.0. The thicknesses of Cu and Co are estimated to be 0.945 and 1.135 nm, using r_{BA}=1.2 and L=2.08 nm. It must be notified that r'_{BA} (=$1/r_{BA}$=0.833) also gives the same peak intensities for t=0 and C_A=1.0. Namely, another possible solution is that the thicknesses of Cu and Co are 1.135 and 0.945 nm.

Table 1 Comparison of the observed and calculated relative (00l) peak intensities in the Cu/Co multilayer.

	Relative Intensities	
l	Observed	Calculated
1	100.0	100.0
2	1.91	2.08
3	8.7	10.0
4	0.17	2.06

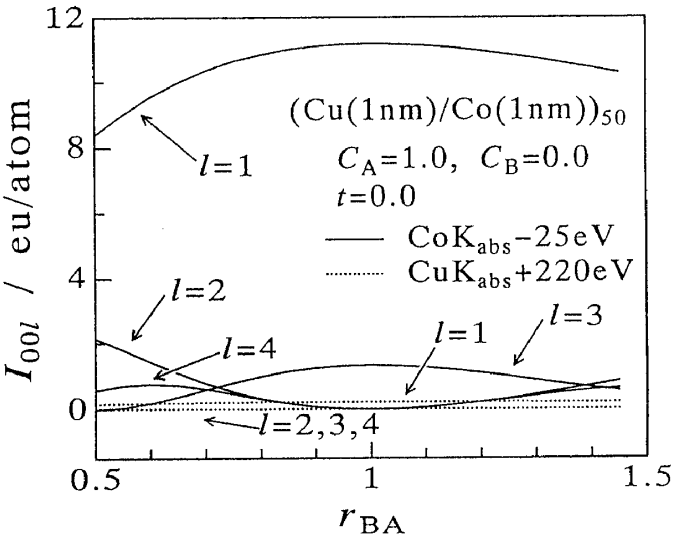

Figure 5 Intensities of the first 4 (00l) peaks for the Cu/Co multilayer as a function of r_{BA} at two energies of 25 eV below Co (solid) and 220 eV above Cu K-absorption edge (dotted).

It is seen in this kind of measurement that an error of the integrated intensity may become larger for the peak with a larger background, such as the 004 peak in Figure 6. By combining intensity profiles observed at two energies around Cu and Co K-absorption edges, this ambiguity might be overcome. In

Eq (12), the peak intensities are proportional to the square of the difference of x-ray atomic scattering factors of Cu and Co, $(f_{Cu}-f_{Co})^2$. Thus, the peak intensities drastically change due to the large values of anomalous dispersion of Cu and Co around their K-absorption edges. The square of the difference is shown in the region including both Co and Cu K-absorption edges in **Figure 7**. In this figure, the energy labelled "A" corresponds to the incident energies used in the present measurement, that is, 25 eV below Co K-absorption edge. Incidentally, the energy of Cu Kα-radiation (8.042 keV) is labelled "B". It is expected that the diffraction peaks at the small-angle region would be observed with Cu Kα without any significant difficulty, although the peak intensity is about a half of those at A and the strong Co Kα and Kβ fluorescent radiations are present.

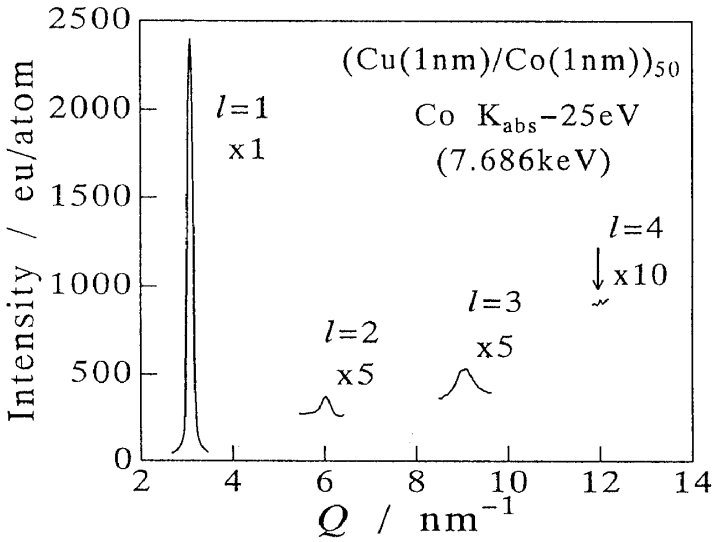

Figure 6 Intensity profiles of (00*l*) peaks in the (Cu(1nm) /Co(1nm))$_{50}$ multilayer observed at 7.686 keV.

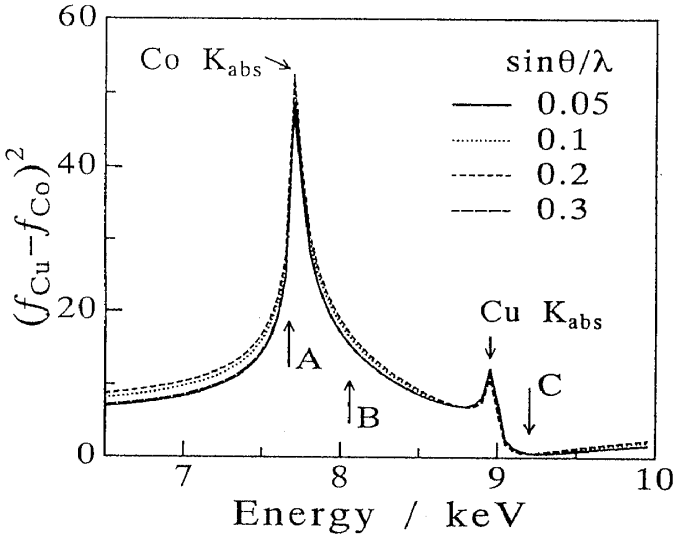

Figure 7 The square of the difference between Cu and Co atomic scattering factors in the energy region including Co and Cu K-absorption edges.

It is also found that the square of the difference becomes almost equal to zero in the energy labelled "C" (9.2 keV) in Figure 7. Thus, the peak intensities at C becomes almost zero. The peak intensities calculated for t=0.0 and C_A=1.0 at C shown with dotted curves in Figure 5 are much smaller than those at A. The intensity profile observed at C may be used as the background profile for calculation of peak intensities at A. This enables us to eliminate the ambiguity in the integrated intensities due to the background intensities. The intensity profiles for the 002 and 003 peaks at C is compared with those at A in **Figure 8**. In the measurement at C, the strong

fluorescent radiations of Cu and Co exist. Thus, in the present measurement at C, the three different intensities from the sample were collected by the Ge solid state detector. Namely, (1) the Co Kα radiation, (2) the Co Kβ and Cu Kα radiations, and (3) the Cu Kβ radiation and the elastic scattering. As explained in the correction for Co Kβ radiation in the measurement at A in the experimental section, the fluorescent radiation overlapping with the elastic radiation was corrected by using the intensity ratios of Co Kβ to Co Kα and Cu Kβ to Cu Kα. The scattering intensity profiles for 002 and 003 peaks at these two energies are shown in Figure 8. More counts at C must be collected in order to improve the counting statistics for estimating the difference. Nevertheless, it is strongly suggested in this figure that this differential method may be used for determining the background intensity.

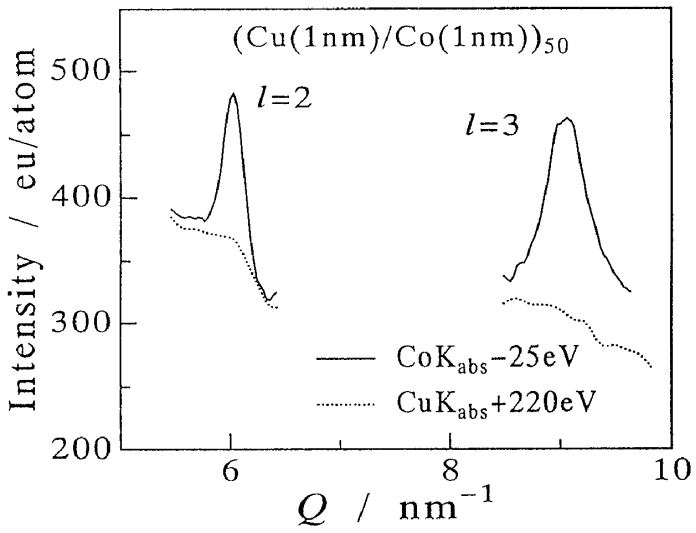

Figure 8 Intensity profiles of 002 and 003 peaks of the Cu/Co multilayer observed at two energies of 25 eV below Co K-absorption edge (solid) and 220 eV above Cu K-absorption edge (dotted).

V. Concluding Remarks

The small angle scattering measurement in reflection geometry becomes a common technique for characterizing the structures of synthesized multilayers. Simultaneously, the quantitative analyses which will provide us more details of the multilayer structure are strongly required. For this purpose, several problems must be solved beforehand. An appropriate method to convert the observed intensity into the intensity in absolute units, which gives us direct information about electron density modulation across the layer by the Fourier transformation. One of the possible methods shown in this paper is to use the monitor counts of the ionization chamber placed just in front of the counter. The first step is to derive the intensity equations for analysis. The second step is to find a way to convert observed intensities into the absolute scale. One of the possible methods has given in this paper. Also, as demonstrated in this paper, the use of the anomalous x-ray scattering may be one way to overcome the difficulties of multilayers by increasing a contrast of x-ray scattering power of the components including next neighboring elements in the periodic table.

Acknowledgements

The authors are grateful to the staff of the Photon Factory, National Laboratory for High Energy Physics, Tsukuba, Particularly, Prof. M. Nomura and Dr.A.Koyama who made the AXS measurement under the proposal No.92-121 possible by their kind service and valuable advice. The $(Cu(1nm)/Co(1nm))_{50}$ multilayer used in the present measurement was provided by Dr. K. Inomata, Toshiba Research and Development Center.

References

(1) M.N.Baibich, J.M.Broto, A.Fert, F.Nguyen Van Dau, F.Petroff, P.Eitenne, G.Creuzet, A.Friederich and J.Chazelas, Phys. Rev. Lett., **61** (1988), 2472.

(2) D.H.Mosca, F.Petroff, A.Fert, P.A.Schroeder, W.P.Pratt,Jr. and R.Laloee and S.Lequien, J. Magn. Magn. Mater., **94** (1991), L1.

(3) S.S.P.Parkin, R.Bhadra and K.P.Roche, Phys. Rev. Lett., **66** (1991), 2152.

(4) N.Nakayama, I.Moritani, T.Shinjo, Y.Fujii and S.Sasaki, J. Phys. F: Met. Phys., **18** (1988), 429.

(5) Y.Saito and K.Inomata, Japan. J. Appl. Phys., **30** (1991), L1733.

(6) N.V.Rao, S.B.Reddy, G.Satyanarayana and D.L.Sastry, Physica C, **138** (1986), 215.

(7) E.Matsubara, K.Harada, Y.Waseda and M.Iwase, Z.Naturforsch., **43a** (1988), 181.

(8) E.Matsubara, Y.Waseda, M.Mitera and T.Masumoto, Trans. Japan Inst. Metals, **29** (1988), 697.